International Journal of GEOMATE, Sept., 2019 Vol.17, Issue 61, pp. 28 - 34
ISSN: 2186-2982 (P), 2186-2990 (O), Japan, DOI: https://doi.org/10.21660/2019.61.4576
Special Issue on Science, Engineering & Environment

HOLE ACCUMULATION EFFECT OF InGaAs HIGH-ELECTRON-MOBILITY TRANSISTORS WITH A 1550-nm WAVELENGTH FEMTOSECOND PULSE LASER

Taiki Kozakai[1], Itsuki Takagi[1], Shun Nakajima[1], and *Hirohisa Taguchi[1]

[1]Department of Electrical and Electronic Engineering, School of Engineering, Chukyo University, Japan

*Corresponding Author, Received: 28 Nov. 2018, Revised: 17 Jan. 2019, Accepted: 06 Feb. 2019

ABSTRACT: InGaAs is known as a material system with high electron mobility derived from InAs and can be formed by metal organic chemical vapor deposition. The base material substrate is InP and is formed by controlling the composition ratio of In and Ga to lattice match with this InP. The bandgap energy Eg of InGaAs is 0.87 eV, and photoelectric conversion of 1550-nm light, which is a communication wavelength band, can be executed. Therefore, it is now used as a detector material in optical communication technology. In this study, we investigated the photoresponsive properties of InGaAs high-electron-mobility transistors (HEMTs) with simultaneous utilization of photoresponse characteristics and high-frequency response characteristics of this InGaAs crystal. A 1550-nm wavelength femtosecond pulse laser (with a pulse width of 100 fs and a period of 50 MHz) was coupled with DC light with a wavelength of 1480 nm and irradiated from the InGaAs HEMT metal electrode surface. Laser light transmitted through the side of the gate metal electrode into the device structure generates electron-hole pairs via the photoelectric effect in the InGaAs layer, and it was confirmed that the maximum drain current of 0.4 mA was reduced. A current response is detected inside the semiconductor by transporting electrons to the drain electrode side and holes to the source electrode side. Because the laser used is pulsed light, the process of generation and disappearance of electron-hole pairs were confirmed as photoresponsive properties.

Keywords: InGaAs HEMT, Photoresponsive property, Photoelectric effect, Hole accumulation effect

1. INTRODUCTION

GaAs is an indispensable material in our current advanced information society [1-3]. GaAs crystal does not exist in a stable in nature, it is most artificially constructed crystal. Stable crystal structure at room temperature is zinc blend type. To use a GaAs semiconductor characteristic effectively, made of a thin film structure on a semiconductor substrate using Metal Organic Chemical Vapor Deposition (MOCVD). GaAs has higher electron mobility than as a general semiconductor Si. It is used as a base material of key devices for transmitting and receiving packet communications in mobile terminals [4]. Because GaAs is used for transmitting and receiving devices, the operating frequency has been dramatically expanded [5]. However, because of the demand for increasing amounts of information, further increases in transmission and reception speeds are required, and situations, where it is difficult to use GaAs, are approaching [6]. It is essential to develop new material systems. InGaAs, a ternary material, has been a subject of focus for a long time [7,8]. InGaAs is known as a material system with high electron mobility derived from InAs and can be to be formed by metal organic chemical vapor deposition [9]. The base material substrate is InP and is formed by controlling the composition ratio of In and Ga to lattice match with this InP. The bandgap energy Eg of InGaAs is 0.87 eV, and photoelectric conversion of 1550 nm light, which is a communication wavelength band, can be executed [10]. Therefore, it is now used as a detector material in optical communication technology [11].

In this study, we investigated the photoresponsive properties of InGaAs high-electron-mobility transistors (HEMTs) with simultaneous utilization of photoresponse characteristics and high-frequency response characteristics of this InGaAs crystal. A 1550-nm wavelength femtosecond pulse laser (with a pulse width of 100 fs and a period of 50 MHz) was coupled with a DC light with a wavelength of 1480 nm and irradiated from the InGaAs HEMT metal electrode surface. Laser light transmitted through the side of the gate metal electrode into the device

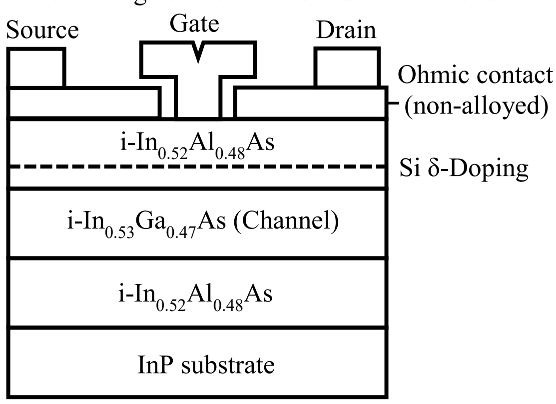

Fig. 1 Schematic cross section of the HEMTs

structure generates electron-hole pairs by the photoelectric effect in the InGaAs layer. The significance of this research is the possibility of HEMT which is an active device to be a passive device.

A current response is detected inside the semiconductor by transporting electrons to the drain electrode side and holes to the source electrode side. Because the laser used is pulsed light, the process of generation and disappearance of electron-hole pairs were confirmed as photoresponsive properties. These results suggest that InGaAs HEMTs may function not only as electronic response devices but also as photoresponsive devices. In this research, we focused on the hole accumulation effect inside the InGaAs layer. By using this effect, a prediction model was constructed regarding the carrier behavior inside the InGaAs layer when the light was irradiated from the device electrode face of the InGaAs HEMT. This model enables the visualization of the hole behavior during InGaAs, optical response of InGaAs HEMT that has been inferred that a hole dominant. These results suggest that InGaAs HEMTs may function not only as electronic response devices but also as photoresponsive devices.

2. EXPERIMENTAL METHOD

Figure 1 shows the crystal structure cross-section of the InGaAs-based HEMT used in this study. The current frequency band of InGaAs is at the 12-GHz level, and it is intended for satellite communication. Therefore, the mounting line was a micro split line with a coplanar structure. The channel layer, InGaAs was lattice-matched with InP substrate and which was sandwiched InAlAs layer. Due to the surface potential difference between InAlAs and InGaAs, a square well potential is formed in the InGaAs layer. Si was sheet-doped in the InAlAs layer on the InGaAs layer. The doping density adjusted to around 1E-12 / cm^2. The number of electrons introduced into the InGaAs layer is larger than the state density function due to the influence of this high concentration doping. As a result, the degeneracy of electronic level occurred inside the InGaAs layer. The two-dimensional electron gas (2DEG) formed due to the degeneracy effect and high-speed operation became possible.

Figure 2 shows the measurement block diagram. An AF4B125 laser (Anritsu Corporation) was used as a direct current laser. The femtosecond pulse laser (Karma Corporation) had a pulse width of 100 fs, a period of 50 MHz, and an average output of 20 mW. These two lasers were polymerized with an optical coupler, and the light intensity was controlled by the direct light intensity. The multiplexed light was split by the optical splitter into an output of 10:90. The 10% output was monitored with a light intensity meter and the remaining 90% was converted to a parallel-plate beam via a drum lens. The incident light output was changed by CW laser. The electrode surface of the InGaAs HEMT had the InAlAs layer of the ohmic contact layer and the Si sheet-doped layer. In this experiment, the wavelength of the pulsed laser light was 1550 nm. The energy of the laser had lower than the band gap energy of the ohmic contact layer and the InAlAs layer. Therefore, 1550 nm light could transparent the two semiconductor layers. External quantum efficiency correspondingly reduced for the electrode metal surface reflections. Nevertheless, a laser could introduce into the InGaAs layer from between the electrodes. The top of the InGaAs HEMT electrode was irradiated via an aerial transition process and the photoresponsive characteristics were confirmed. For the measurement, a network analyzer at the 40-GHz level (Anritsu MS4664B) was used. A single-mode fiber was used for the light transmission

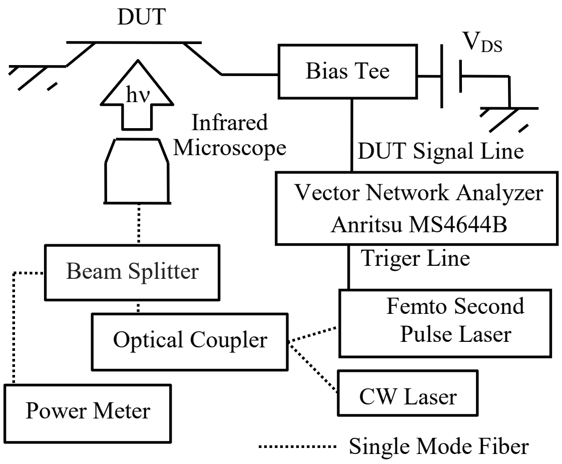

Fig. 2 Measurement block diagram

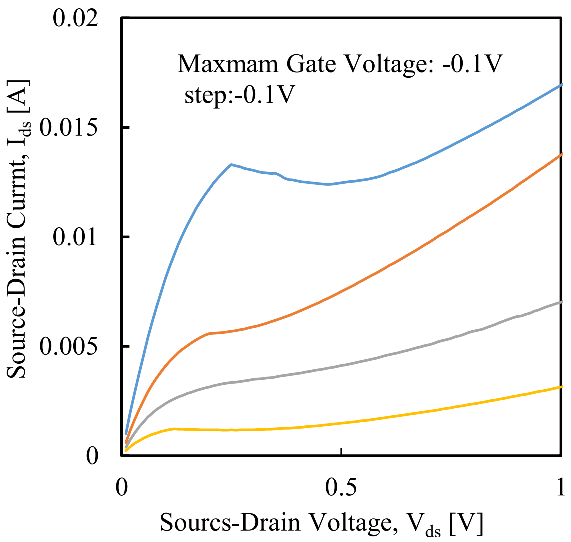

Fig. 3 DC characteristic of an InGaAs HEMT

path. For the high-frequency-response measurement, a 40-GHz-level adaptation system was used.

3. RESULTS AND DISCUSSION

3.1 DC Characteristics of InGaAs HEMTs

Figure 3 shows the DC current-voltage characteristics (*IV* characteristics) of the InGaAs HEMT used this time. As shown in fig. 1, the gate portion of the InAlAs layer does not have a recess structure. Therefore, InGaAs HEMT shows of depletion type IV characteristics. In order to completely turn off the channel current of this type of HEMT, it is necessary to greatly negative the gate voltage. This type of characteristic is not suitable for switching operation. However, InAlAs layer does not carry out the manufacturing process in the direction perpendicular to the gate part, which ensures high reliability in device characteristics and lifetime. In addition, a stable current amplification factor can be obtained. Although a relatively good drain current rise is seen in the linear region, the current does not exhibit a complete saturation state in the saturated region but rather a slightly rising upward characteristic. For this reason, the drain conductance Gd has a certain value or more, but the transconductance Gm has a good value of 100 S.

3.2 Confirmation and Analysis of Photoresponse Characteristics

Clear optical response characteristics were confirmed in the *IV* characteristics of Fig. 3. At the stage when the coupling light entered the HEMT, the drain current value was reduced by 0.4 mA at the maximum. To clarify that this lowering phenomenon is a photoresponsive characteristic, the S parameter was measured by a vector network analyzer (Anritsu MS4644B) and a parameter analysis was conducted.

Figure 4 shows the frequency dependence characteristics of the source-gate capacitance C_{gs} and the gate-drain capacitance C_{dg}. The light output was controlled by CW laser output. The output intensity was 50 mW, 72 mW, 90 mW. This is the incident light output on the top of InGaAs-HEMT. In Fig. 4, the blue line shows the frequency dependence before light irradiation and other lines show the frequency dependency during light irradiation. Slight decreases in both C_{gs} and C_{gd} induced by light irradiation can be seen. Electron-hole pairs should have been generated in the InGaAs layer by light irradiation. Photogenerated electrons are transported to the drain side together with a two-dimensional electron gas (2DEG). Both C_{gs} and C_{gd} values are confirmed to be clearly degraded by light irradiation. However distinct changes are only at 50mW light irradiation before the light irradiation (0 mW). No clear light intensity dependence has been confirmed during light

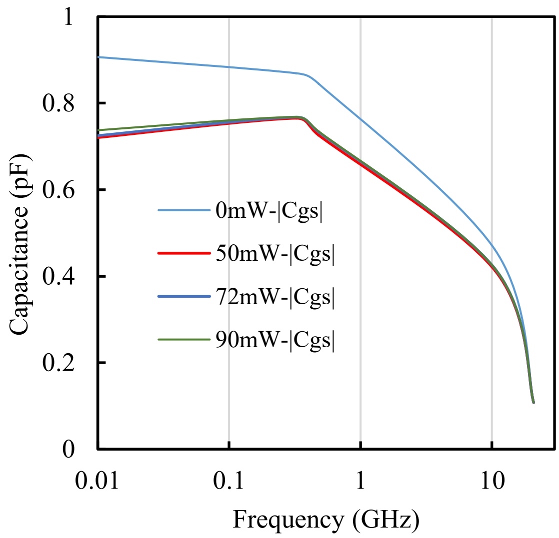

(a)

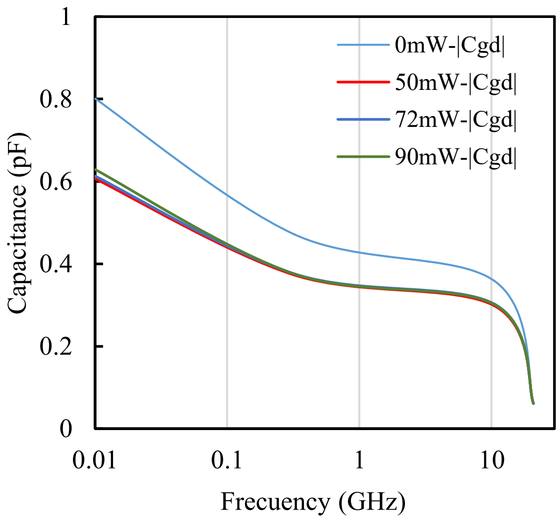

(b)

Fig. 4 Frequency dependence characteristics of the parasitic capacitance of InGaAs HEMT

(a) Source–gate capacitance, C_{gs}
(b) Gate–drain capacitance, C_{dg}

irradiation. It is obvious that electron-hole pairs were generated in the InGaAs layer by light irradiation. Although it increased the light intensity, it did not have a large change in the electron-hole pairs generation rate. Next, the current amplification factor is confirmed whether it has changed by ON/ OFF of light irradiation. Figure 5 shows the frequency dependence of the current gain before and after light irradiation. There is almost no difference before and after. It is thought that the gain current was as weak as 0.4 mA at the maximum and was not reflected in the h21 parameter. From fig. 5, it is considered that the number of electron-hole pairs generated by light irradiation is extremely small. In this experimental system, the window for introducing the laser light into the InGsaAs layer is only the gap existing between the source and gate electrodes or the gap existing between the gate and drain electrodes. In addition, a three-layer structure of Ti / Pt / Au is formed as a gate metal, and both are materials having a metallic luster. Radiation light reflection from Au on the surface and reflection from Ti / Pt on the electrode side surface. It is thought that these deteriorated external quantum efficiencies, resulting in weak photocurrent.

Figure 6 shows the frequency dependence characteristic of the drain conductance G_d. A clear difference was confirmed for G_d depending on the presence or absence of light irradiation. It was confirmed that the drain conductance was lowered by light irradiation. Moreover, contrary to the results of capacitive component analysis and gain analysis, the drain conductance is confirmed to be slightly dependent on the light intensity. A phenomenon that does not affect the current value change rate and the parasitic component is expressed inside the InGaAs layer. In addition, the decrease of Gd suggests the existence of the electron consumption process inside the channel. The reason for this will be discussed below.

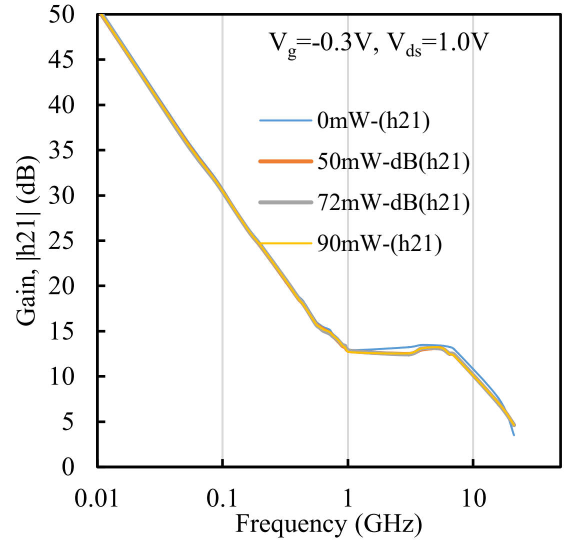

Fig. 5 Frequency dependence of the current gain before and after light irradiation

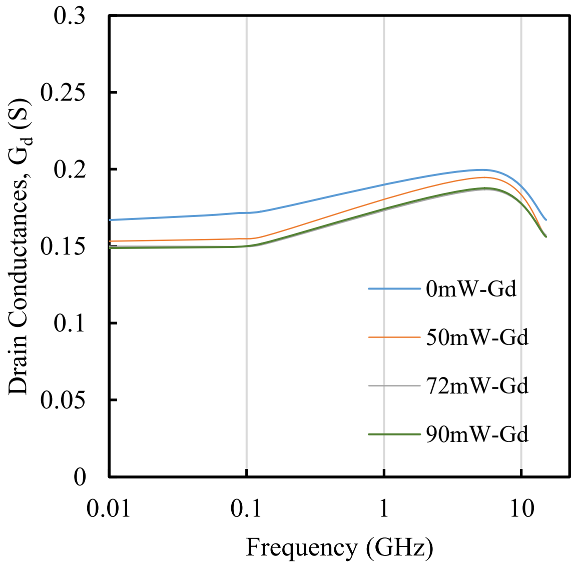

Fig. 6 Frequency dependence characteristic of the drain conductance G_d

3.3 Hole Accumulation Effect

It is known that the InGaAs layer originally has a hole accumulation effect [12]. At this time, holes are accumulated in the InGaAs between the gate and the source. The accumulated holes are recombined with a 2DEG, attenuating the number of transferred electrons, and this attenuation is a frequency dispersion phenomenon of G_d. [13,14]. Based on this hole accumulation effect, consider what phenomenon has occurred in the device in which the InGaAs-HEMT channel layer. Expectations diagram for carrier behavior within the InGaAs HEMT device shown in figure 7. First, figure 7 (a) shows carriers in the channel layer in the case without light irradiation. At this time, the electrons supplied from the source move inside the two-dimensional electron gas located under the InAlAs layer and the InGaAs layer and go out to the drain electrode.

Next, figure 7 (b) shows the carrier inside the device during light irradiation. By executing light irradiation, thermal vibration occurs due to an increase in energy inside the device, and the bonds between atoms are broken. Electron-hole pairs are generated by photovoltaic effect [15]. The generated electrons move in the two-dimensional electron gas and reach the drain electrode side. Holes form two-dimensional hole gas (2DHG) in the lower part of the InGaAs layer and move to the source electrode side [16]. In InGaAs-HEMT devices, heterojunction plane by InAlAs and InGaAs has two sides vertically sandwiching the InGaAs layer has a structure that confines the carriers, respectively. Two-dimensional electron gas (2 DEG) is formed on the upper surface of the InGaAs layer and two-dimensional hole gas (2 DHG) is formed on the lower InGaAs surface. Figure 7 (b) and (c), 2DHG shows a layer of orange. Here, the hole cannot go out and from the outside using the source electrode. The source electrode is located on the 2DHG layer opposite direction, the potential barrier possessed by the InAlAs inhibit hole transport. It is known from this that hole accumulation occurs between the source and the gate as shown in fig. 7 (c) [17, 18]. Here, as the light irradiation is continued, the amount of hole accumulation continues to increase. When this hole reaches the 2DEG layer, recombination occurs with electrons in the layer. A large number of holes generated by hole accumulation effect is known to perform Auger recombination [19, 20]. Recombination within the normal InGaAs layer indicates band-to-band recombination and creates a light emission mode [21]. However, when the number of holes exceeds a certain value, the non-emission Auger recombination mode dominates the main factor. It is known that the hole consumption rate due to Auger recombination is a higher speed mode than band recombination [22]. Thus, the electron density of the 2DEG is rapidly decreased. This effect contributed to the decrease of the source-drain current value during light irradiation. Also, while the drain conductance varies depending on the presence or absence of light irradiation, the reason why Gain did not change can also be explained by the hole accumulation effect. From the above, it is concluded that the photoresponse of the InGaAs-HEMT device in this study is a hole response.

4. CONCLUSIONS

A 1550-nm wavelength femtosecond pulse laser (with a pulse width of 100 fs and a period of 50 MHz) and DC light with a wavelength of 1480 nm were coupled to an InGaAs HEMT and irradiated from the device metal electrode surface. Semiconductor laser light penetrating into the device structure from the side surface of the gate metal electrode generated electron-hole pairs by the photoelectric effect in the InGaAs layer, and it was confirmed that the maximum drain current of 0.4 mA was reduced. In electron-hole pairs generated by incident light holes accumulated in the source region. It is clear from the S parameter analysis that the hole accumulation effect is due to noticeable frequency dispersion of the drain conductance. These results suggest that InGaAs HEMTs may function not only as electronic response devices but also as photoresponsive devices. In this research, we focused on the hole accumulation effect inside the InGaAs layer. By using this effect, a prediction model was constructed regarding the carrier behavior inside the InGaAs layer when the light was irradiated from the device electrode face of the InGaAs HEMT. This model enables the visualization of the hole behavior during InGaAs, optical response of InGaAs HEMT that has been inferred that a hole dominant.

From now on, we will investigate system-on-chip of photoresponsive element and signal processing element on InGaAs crystal.

5. ACKNOWLEDGMENTS

The authors are grateful to the Chukyo University Research Found for financial assistance with this research.

6. REFERENCES

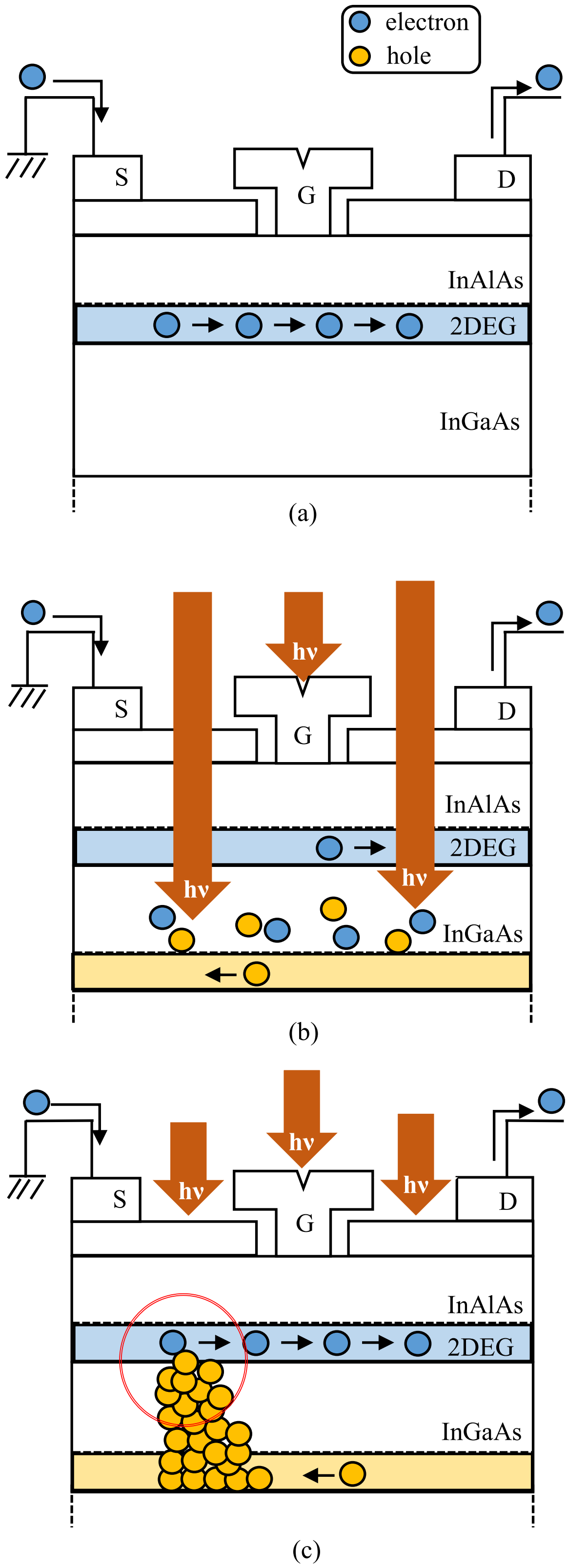

Fig. 7 Expectations diagram for carrier behavior within the InGaAs HEMT

(a) Without light irradiation
(b) Device during light irradiation
(c) Hole accumulation effect

[1] Shur M.S., Low Ballistic Mobility in Submicron HEMTs, IEEE Electron Device Letters, Vol. 23, Issue 9. 2002, pp. 511–513.

[2] Salis G., Semiconductor spintronics: switching spins at low voltage, Proceedings of the 2013 International Symposium on Low Power Electronics and Design, 2013, pp. 143.

[3] Chinni V. K., Zaknoune M., Coinon C., Morgenroth L., Troadec D., Wallart X., and Desplanque L., V-Shaped InAs/Al0.5Ga0.5Sb Vertical Tunnel FET on GaAs (001) Substrate With ION = 433 μA.μm−1 at VDS = 0.5 V, IEEE Journal of the Electron Devices Society, Vol.3, NO. 3, 2017, pp. 53-58.

[4] Aberle J.T., Oh S. H., Auckland D.T., and Rogers S.D., Reconfigurable antennas for wireless devices, IEEE Antennas, and Propagation Magazine, Vol. 45, Issue, 6, 2003, pp. 148–154.

[5] Yuan Y., Fan Y., Chen Z., Li L., and Yang Z., Ku Band 2 Watt TR Chip for Phased Array Based on GaAs Technology, IEICE Electronics Express, Vol. 13, Issue 7, 2016, pp. 1–6.

[6] Taguchi H., Murakami H., Oura M., Iida T., and Takanashi Y., Analysis of Deviation of Threshold Voltage from Hole Accumulation Model, Japanese Journal of Applied Physics, Vol. 45, No. 11, 2006, pp. 8549–8555.

[7] Tayel M. B., Yassin A. H., Parameters Extraction for Pseudomorphic HEMTs Using Genetic Algorithms, Proceedings of 2009 International Conference on Electronic Computer Technology, 2009, pp 600-603.

[8] Otsuki K., Kainuma Y., Miyashita R., Yamanaka K., and Taguchi H., DC and RF Characteristics Fluctuation of InAlAs/InGaAs HEMTs, International Journal of GEOMATE, Vol. 12, Issue 34, 2017, pp. 28–31.

[9] Kawasaki T., Sugawara K., Dobroiu A., Wako H., Watanabe T., Suemitsu T., Ryzhii V., Iwatsuki K., Kuwano S., Kani J., Terada J., and Otsuji T., InGaAs Channel HEMTs for Photonic Frequency Double Mixing Conversion over the Sub-THz Band, Proceedings of 2015 IEEE MTT-S International Microwave Symposium (IMS), 2015, pp. 1-4.

[10] Li G., Guo T., Zhang H., Gao H., Zhang J., Liu B., Yuan S., Kai G., and Dong X., Fiber grating sensing interrogation based on an InGaAs photodiode linear array, Applied Optics, Vol. 46, No. 3,2007, pp. 283-286.

[11] Zhang J., Itzler M.A., Zbinden H., and Pan J.W., Advances in InGaAs/InP Single-photon Detector Systems for Quantum Communication, Light: Science & Applications, Vol. 4, e286, 2015, pp. 1–15.

[12] Taguchi H., Kawaguchi M., Hayakawa M., Nakamura Y., Iida T., and Takanashi Y., Frequency Dependence of Drain Conductance due to Hole Accumulation in InAlAs/InGaAs High Electron Mobility Transistors, Japanese Journal of Applied Physics, Vol. 45, Part 1, Number 6A, 2006, pp. 4960–4967.

[13] Taguchi H., Sato T., Oura M., Iida T., and Takanashi Y., Dependence of Carrier Lifetime of InAlAs/InGaAs High Electron Mobility Transistors on Gate-to-Source Voltage, Japanese Journal of Applied Physics, Vol. 47, No. 4, 2008, pp. 2858–2861.

[14] Nakano S. and Taguchi H., Analysis of Intrinsic Delay Time in InAlAs/InGaAs High-Electron-Mobility Transistors at Cryogenic Temperature, Proceedings of IEEE TENCON2017, 2017, pp. 1685–1689.

[15] Beeler R., Mathews J., Weng C., Tolle J., Roucka R., Chizmeshya, Juday A.V.G. R., Bagchi S., Menéndez J., Kouvetakis J., Comparative study of InGaAs integration on bulk Ge and virtual Ge/Si(1 0 0) substrates for low-cost photovoltaic applications, Solar Energy Materials and Solar Cells, Vol. 49, No. 12, 2010, pp. 2362-2370.

[16] Wunderlich J., Kaestner B., Sinova J., and Jungwirth T., Experimental Observation of the Spin-Hall Effect in a Two-Dimensional Spin-Orbit Coupled Semiconductor System, Phys. Rev. Lett. Vol. 94, No. 4, 2005, pp. 047204.

[17] Choi C. S., Kang H. S., Choi W. Y., Kim H. J., Choi W. J., Kim D. H., Jang K. C., Seo K. S., High optical responsivity of InAlAs-InGaAs metamorphic high-electron mobility transistor on GaAs substrate with composite channels, IEEE Photonics Technology Letters, Vol. 15, NO. 6 , 2003, pp. 846 – 848.

[18] Kang, H.S. Choi C.S., and Choi W.Y., Characterization of phototransistor internal gain in metamorphic high electron mobility transistors, Applied Physics Letters, Vol. 84, No. 19, 2004, pp. 3780-3782.

[19] Hausser S., Fuchs G., Hangleiter A., and Streubel K., Auger recombination in bulk and quantum well InGaAs, Applied Physics letter, Vol. 56, No.10, 1989, pp. 913-916.

[20] Binder M., Nirschl A., Zeisel R., Hager T., Lugauer H.J., Sabathil M., Bougeard D., Wagner J., and Galler B., Identification of nnp and npp Auger recombination as significant contributor to the efficiency droop in (GaIn)N quantum wells by visualization of hot carriers in photoluminescence, Applied Physics letter, Vol. 103, No.7, 2013, pp. 071108-1-5.

[21] Smets Q., Verreck D., Verhulst A. S., Rooyackers R., Merckling C., Put M. V. D.,

Simoen E., Vandervorst W., Collaert N., Thean V. Y., Sorée B., Groeseneken G., and Heyns M. M., InGaAs tunnel diodes for the calibration of semi-classical and quantum mechanical band-to-band tunneling models, Journal of Applied Physics Vol. 115, No. 18, 2014, pp. 18403-1-9.

[22] Fathpour S., Mi Z., Bhattacharya P., Kovsh A. R., Mikhrin S. S., Krestnikov I. L., Kozhukhov A. V., and Ledentsov N. N., The role of Auger recombination in the temperature-dependent output characteristics (T_0= ω)of p-doped 1.3 µm quantum dot lasers, Applied Physics Letters, Vol.85, No. 22, 2004, pp. 5164-5166.